C-H Activation of Fluoroarenes: Synthesis, Structure and Luminescence Properties of Cu(I) and Au(I) Complexes Bearing 2-Phenylpyridine Ligands

Roberto Molteni, Katharina Edkins,† Martin Haehnel, and Andreas Steffen*

Institut für Anorganische Chemie, Fakultät für Chemie und Pharmazie, Universität Würzburg, Am Hubland, 97074 Würzburg, Germany

d^{10} metal complexes – phenylpyridine – phosphorescence – copper – fluorine – C-H activation – gold

ABSTRACT: Although 2-phenylpyridine (ppy)-type have been employed very successfully for the design of luminescent Ir^{III} and Pt^{II} complexes, corresponding d^{10}-coinage metal complexes are unknown. We report on the synthesis of the first, at room temperature stable, Cu^{I} 2-phenylpyridine (ppy)-type complexes, by C-H activation of 2-(2,3,4,5-tetrafluorophenyl)pyridine (Htfppy, **1**) using [Cu(OH)(IDipp)] (**2**) (IDipp = bis(2,6-di-isopropylphenyl)imidazole-2-ylidene), or by lithiation of **1** and subsequent reaction with $CuBr{\cdot}SMe_2$ in the presence of POP ligand (POP = bis{2-(diphenylphosphanyl)phenyl}ether) in THF, giving [Cu(tfppy)(IDipp)] (**3**) or [Cu(tfppy)(POP)] (**4**). The complexes thus obtained adopt distorted trigonal and tetrahedral coordination geometries, respectively. Gold(I) tfppy complexes with IDipp (**5**) or $PTol_3$ (**6**) ligands have also been prepared, showing a preference for linear coordination environments due to the non-coordinating pyridine moiety of the tfppy ligand. These structural differences have a profound effect on the photophysical properties of the coinage metal ppy compounds. The Cu^{I} tfppy complexes exhibit intense orange-red luminescence (λ_{max} = 610 (**3**), 607 (**4**) nm) from a ^{3}(intra-ligand)CT state in the solid state at room temperature, with phosphorescence lifetimes of τ = 8.6 (**3**) and 9.5 (**4**) μs. In contrast, the linear coordination leads to weak emission of the Au^{I} complexes, with **5** displaying simultaneous fluorescence and phosphorescence. Surprisingly, reaction of **2** with Htfppy (**1**) in MeCN leads to solvent activation and to isolation of a copper acetamide complex [Cu(N(H)C(O)Me)(IDipp)] (**14**).

I. INTRODUCTION

2,2′-Bipyridine (bpy) and 2-phenylpyridine (ppy), and derivatives thereof, are among the most widely used ligands for photoactive d^6 and d^8 transition metal complexes, which have been exploited in photocatalysis, organic light emitting diodes (OLEDs), light emitting electrochemical cells (LEECs) and biomedical applications.[1-13] In particular the prototypical complexes $[Ru(bpy)_3]^{2+}$ and $[Ir(ppy)_3]$ have received great attention in fundamental photophysical studies, which subsequently led to their employment in solar energy conversion and OLEDs, respectively, and the resulting progress in those areas underlines the importance of such compounds.[14-15]

In the last few years, d^{10} copper(I) complexes have emerged as potentially superior materials for the design of highly efficient emitters in OLEDs in comparison to compounds based on d^6 or d^8 transition metals.[16-17] This is, on the one hand, due to the absence of metal centered d-d* transitions in d^{10} systems, which can provide undesired pathways of non-radiative decay. On the other hand, Cu^{I} complexes can display thermally activated delayed fluorescence (TADF), i.e. thermal repopulation of the singlet excited state S_1 from the triplet excited state T_1, greatly enhancing the radiative rate constant.[18-23] Despite the comparably weak spin-orbit coupling (SOC) of Cu^{I} (ζ_{Cu} = 829 cm^{-1}, ζ_{Ir} = 3909 cm^{-1}), which has previously been seen as the main advantage of Ir^{III}-based luminophores, this process allows to indirectly harvest the triplet states and can give very high luminescence quantum yields, as has been shown recently by Yersin and others.[24-42]

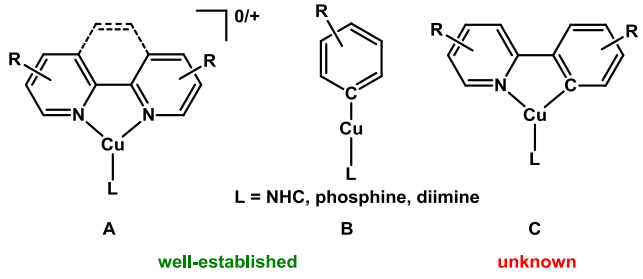

Scheme 1. Known Cu^{I} Diimine and Aryl, and Unknown Copper(I) 2-Phenylpyridine Complexes.

While bpy and its derivatives have been extensively studied as π-chromophore ligands in Cu^{I} NHC, phosphine and diimine compounds of type **A**,[16-17,43] monocopper(I) aryl complexes have been discussed as reactive intermediates in cross-coupling reactions, such as the Ullman coupling, and some linear coordinated type **B** species have even been isolated (Scheme 1).[44-68] Interestingly, no studies on the photophysical properties of linear copper(I) aryl complexes were published, except for [Cu(C_6F_5)(py)], of which the emission originates from the formation of one-dimensional polymeric chains in the solid state by unsupported Cu-Cu interactions.[59,69-72] In solution, no photoluminescence from the monomers is observed. The lack of photophysical studies on this class of compound is probably due to the fact that, judging from literature reports, trigonal or tetrahedral coordination geometries around the copper(I) center seem to be favorable for achieving efficient phosphorescence.[16-17,24-42,73-74]

So far, only one example of a tetrahedral coordination geometry of a copper(I) aryl has been structurally characterized, which is [Cu(Ph){$MeC(CH_2PPh_2)_3$}],[75] and only a few examples of a trigonal arrangement are known.[69,76-80] Their photophysical properties have not been reported.

In contrast to Cu^{I} diimine and aryl complexes, the analogous compounds with 2-phenylpyridine are still unknown (type **C**, Scheme 1). Indeed, synthetic access to trigonal or tetrahedral Cu^{I} ppy compounds is not trivial, as it would involve regioselective C-H activation in the 2-position of the phenyl moiety. However, it should be possible to bypass this problem by partial fluorination of the aryl ring, increasing the acidity of the C-H bond in the 2-position and at the same time increasing the ionic character of the copper-carbon bond, which should have the beneficial effect of higher stability compared to non-fluorinated aryl ligands at copper(I).

In this work, we report on the successful synthesis and structural characterization of trigonal and tetrahedral Cu^{I} ppy-type complexes, and investigate their luminescence behavior. For comparison, related d^{10} Au^{I} ppy-type complexes have also been prepared, which are, in contrast to their d^{8} Au^{III} analogues, also unknown.[81-83]

II. RESULTS AND DISCUSSION

Synthesis and characterization of Cu^{I} and Au^{I} ppy-type complexes. In order to achieve facile Cu^{I}-C bond formation in the 2-position of the phenyl moiety of ppy-type ligands, we have chosen 2-(2,3,4,5-tetrafluorophenyl)pyridine (Htfppy) (**1**),[84] due to its high C-H acidity and its potential to form stable M-C bonds, to react with [Cu(OH)(IDipp)] (IDipp = bis(2,6-di-*iso*propyl-phenyl)imidazol-2-ylidene) (**2**). Indeed, when the reaction of **1** and **2** is carried out in THF at -40°C, the formation of [Cu(tfppy)(IDipp)] (**3**) occurs in ca. 50 % yield. In the presence of 4 Å molecular sieves, trapping water formed during the reaction, full conversion to trigonal **3** is observed (Scheme 2), which has been characterized by multinuclear ^{1}H, $^{13}C\{^{1}H\}$, $^{13}C\{^{19}F\}$, ^{15}N and ^{19}F NMR spectroscopic studies, MALDI-TOF mass spectrometry, elemental analysis and single-crystal X-ray diffraction studies.

The most pronounced change in the ^{1}H NMR spectrum of the free ligand upon coordination to the Cu^{I} NHC fragment is a 0.83 ppm shift to 7.90 ppm of the C-H functionality *ortho* to the pyridine nitrogen. The ^{19}F NMR spectrum shows a resonance at -105.9 ppm, typical for organometallics bearing fluoroaromatic ligands with a fluorine atom *ortho* to a metal center.[85-89] The C_{ipso} of the IDipp ligand is found at 185.5 ppm in the $^{13}C\{^{1}H\}$ NMR spectrum, while the resonances of the tetrafluorophenyl moiety appear between 150 and 120 ppm, with the typical complex couplings to the fluorine atoms. The C_{ipso} of the tfppy ligand is found in the $^{13}C\{^{19}F\}$ at 123.9 ppm with unresolved coupling leading to observation as a broad singlet. The resonances of the IDipp and tfppy nitrogens are found at -185.9 and -85.7 ppm, respectively, in the ^{15}N NMR spectrum. The pyridine coordination in solution can be deduced by comparison with the ^{15}N resonance of the free ligand **1** at -70 ppm.

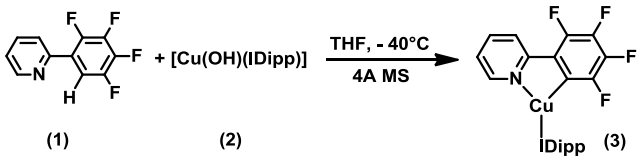

Scheme 2. Synthesis of [Cu(tfppy)(Dipp)] (3) by reaction of 1 with [Cu(tfppy)(Dipp)] (2) in the presence of molecular sieves.

Introduction of phosphine ligands, and thus generation of a tetrahedral coordination geometry around the copper atom, was possible by lithiation of Htfppy (**1**) in the presence of TMEDA at -40°C and subsequent reaction with $CuBr{\cdot}SMe_2$ in the presence of POP (POP = bis{2-(diphenylphosphanyl)phenyl}ether) at room temperature (Scheme 3), giving [Cu(tfppy)(POP)] (**4**). Employing non-chelating phosphines, such as PR_3 (R = Me, Ph) or PPh_2Me, resulted in decomposition in solution and the precipitation of elemental copper.

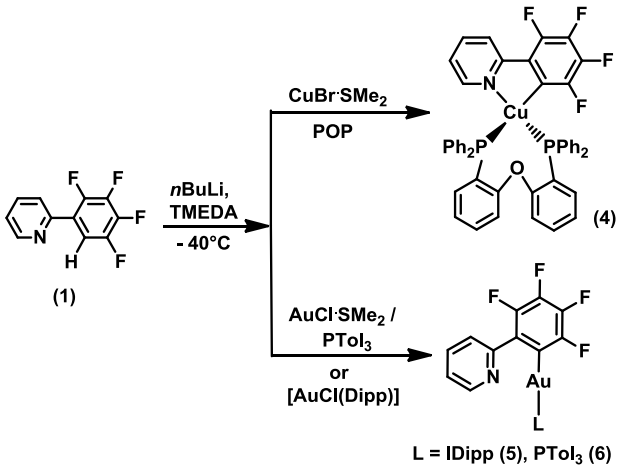

Scheme 3. Synthesis of tetrahedral Cu(I) and linear Au(I) tfppy complexes 4-6 by lithiation of 1.

Apart from the single-crystal X-ray diffraction experiments (see below), the following selected NMR data unambiguously characterize complex **4**. The ^{19}F NMR spectrum of **10** shows a low-field shift of the fluorine in the 5-position of the phenyl moiety to -105.0 ppm. The *ipso*-carbon is found at 128.9 ppm in the ^{13}C{^{1}H} NMR spectrum. The coordination of the pyridine to the copper atom in solution is confirmed by a resonance at -100 ppm in the ^{15}N NMR spectrum, while the ^{15}N resonance of the free ligand is observed at -70 ppm (Figure 1).

The same strategy as for **4** has been employed to obtain Au^{I} complexes bearing ppy-type ligands. Specifically, reaction of Li(tfppy)[87] with [AuCl(IDipp)] or AuCl·SMe$_2$, in the presence of PTol$_3$, yields the linear coordinated complexes [Au(tfppy)(IDipp)] (**5**) and [Au(tfppy)(PTol$_3$)] (**6**), respectively. We found the *ipso*-carbon resonances of **5** and **6** in the ^{13}C{^{19}F} NMR spectra at 149.9 and 154.9 ppm, respectively, which is in a similar range as found for [Au(C$_6$F$_5$)(P*t*Bu$_3$)] (139 ppm).[88] The resonances of the fluorines *ortho* to the gold(I) centers are found in the ^{19}F NMR spectra at -115 and -112 ppm for **5** and **6**, respectively.

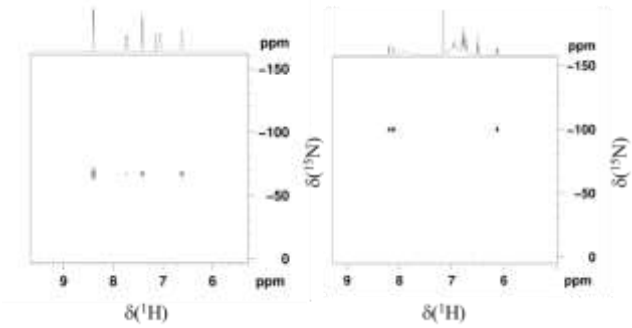

Figure 1. (^{15}N, ^{1}H)HMBC (C$_6$D$_6$, 500 MHz) of free ligand Htfppy (**1**) (left) and [Cu(tfppy)(POP)] (**4**).

2-(2,4-Difluorophenyl)pyridine (**7**) has previously been used for the design of blue light emitting Ir^{III} complexes,[14,89] and thus we investigated the selectivity of C-H activation of **7** with [Cu(OH)(IDipp)] (**2**) (Scheme 4). Pre-coordination *via* the nitrogen atom of the pyridine moiety does not lead to C-H activation in the 6-position of the phenyl moiety, and it seems that the 3-position is favored due to the higher acidity originating from the adjacent fluorine substituents. Although we were not able to grow single-crystals suitable for X-ray diffraction studies, the identity of [Cu(3-dfppy)(IDipp)] (**8**) has been confirmed by comparison of the ^{1}H, ^{13}C and ^{19}F NMR spectra with those of the free Htfppy ligand (**1**), and the copper complexes **3** and **4**. While the ^{13}C resonance of the 3-position of the 2,4-Difluorophenyl ring is found at 132.25 ppm, it shifts upon binding to Cu^{I} in **8** to 130.1 ppm; this C_{ipso} is only observable in the ^{13}C{^{19}F}, and not in the ^{13}C{^{1}H} NMR spectrum. The two remaining C-H functionalities of the phenyl ring, giving rise to ^{13}C resonances at 109.1 and 128.9 ppm, do not show any $^{2}J_{CF}$, in agreement with the proposed structure. In addition, their signals in the ^{1}H NMR spectrum show $^{3}J_{HH}$ coupling of 8 Hz, typical for hydrogens in *ortho* position. The ^{19}F NMR spectrum of **8** gives two resonances at -82.7 and -84.9 ppm, which means a shift of over 25 ppm in comparison with the free ligand dfppy (-110.1 and -113.2 ppm), in agreement both fluorines being in *ortho* position to the metal center.

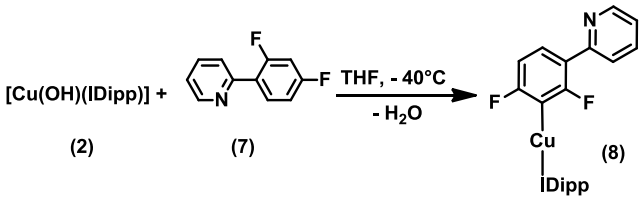

Scheme 4. C-H activation of 2-(2,4-difluorophenyl)-pyridine by [Cu(OH)(IDipp)] (2) giving 8.

Reactivity of [Cu(OR)(IDipp)] (R = H (2), O*t*Bu (10)) with Htfppy (1) in acetonitrile. The choice of solvent and the use of molecular sieves are important issues for the synthesis of [Cu(tfppy)(IDipp)] (**2**) (Scheme 2), as otherwise undesired, albeit interesting, side-reactions occur. For instance, in acetonitrile at room temperature, *in situ* ^{19}F NMR spectroscopic measurements show also immediate formation of the desired product **3** upon dissolving Htfppy (**1**) together with [Cu(OH)(IDipp)] (**2**), but the reaction continues under re-protonation of tfppy by H$_2$O, apparently leading to the formation of [Cu(**1**)(IDipp)](OH) (**9**) as the final product (Scheme 5 and Figures 2, S16 and S17).

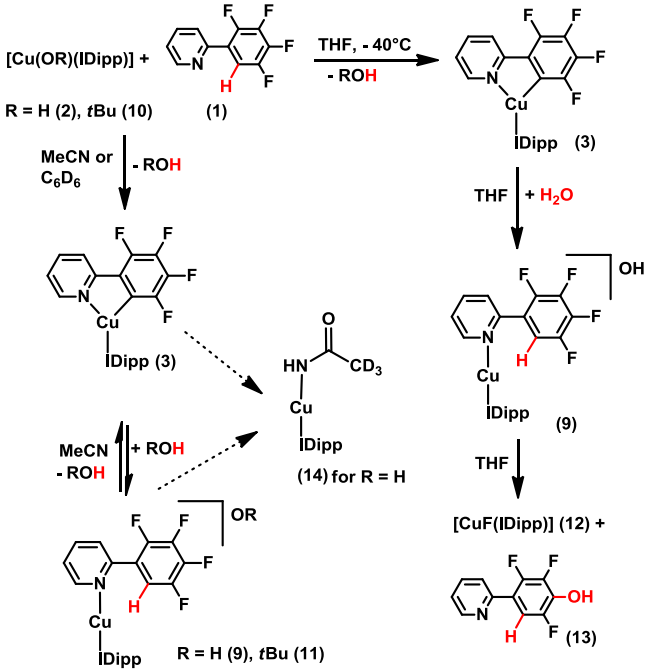

Scheme 5. Reaction of 1 with [Cu(OR)(Dipp)] (R = H (2), *t*Bu (10)) in THF, C$_6$D$_6$ and in MeCN.

The resonance for the fluorine *ortho* to copper in **3** at -105.9 ppm vanishes during the reaction. The *N*-coordinating ligand in **9** gives rise to a small shift in the ^{19}F NMR spectrum of the fluorine *para* to the pyridine by ca. 0.25 ppm (see Figure 2) compared to the free ligand **1**

and ca. 1 ppm compared to **2**, and the complex F-H coupling pattern reappears. All other fluorine resonances do not change. The *in situ* ^{1}H NMR spectrum shows the fluoroarene C-H group in the 2-position at 7.45 ppm, with a complex coupling pattern. While the IR spectrum of **2** shows a typical OH stretching frequency at 3570 cm^{-1}, the *in situ* IR spectrum of the reaction mixture indicates no copper-bound hydroxide (Figures S18 and S19).

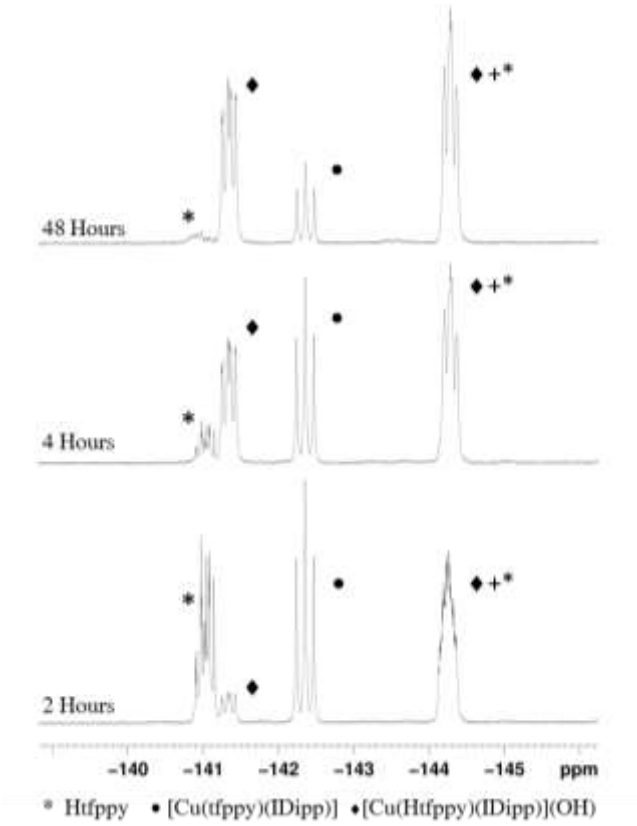

Figure 2. Excerpt of the *in situ* ^{19}F NMR spectrum (CD_3CN, 188 MHz) from the reaction of Htfppy (**1**) with [Cu(OH)(IDipp)] (**2**).

Although an outer-sphere hydroxide is difficult to rationalize and we have no structural proof, its formation is strongly supported by the fact that reaction of [Cu(O*t*Bu)(IDipp)] (**10**) with **1** gives also **3** which, according to NMR spectroscopic studies (Figure S14), subsequently rearranges partially to [Cu(**1**)(IDipp)](O*t*Bu) (**11**), indicating equilibrium between **3** and **11** (Scheme 5). The data for **9** and **11** are identical to an *in situ* NMR study of the reaction of [CuCl(IDipp)] with **1** in the presence of $AgPF_6$, leading to precipitation of AgCl and formation of [Cu(IDipp)(tfppyH)]PF_6 (Figures S20-S23), of which the additional ^{15}N NMR spectrum confirms pyridine *N*-coordination to copper with a resonance at -78.9 ppm. Further indication for the ionic products **9** and **11** formed in MeCN is given by the outcome of the reaction of Htfppy (**1**) and **2** in less polar C_6D_6, which gives only stable [Cu(tfppy)(IDipp)] (**3**) in ca. 30 %, but the conversion does not continue even after 6 days. It should also be mentioned that in THF as a solvent without molecular sieves, protonation and presumably hydroxylation of the tfppy ligand occurs after initial formation of **3** from reaction of **1** with **2**, giving a copper fluoride complex (**12**) and hydroxydefluorinated organic **13** (Scheme 5).

Our attempts to recrystallize **9** from the acetonitrile reaction mixture to confirm its proposed structure led to reproducible isolation of single-crystals of [Cu(N(H)C(O)CD_3)(IDipp)] (**14**) as a byproduct, which is the result of a formal hydroxylation of copper(I) bound MeCN (Figure 3, Scheme 5). The amide N-H resonance is found at 2.17 ppm in the ^{1}H NMR spectrum, while the CD_3 group gives rise to a singlet at 1.09 ppm in the ^{2}H NMR spectrum.

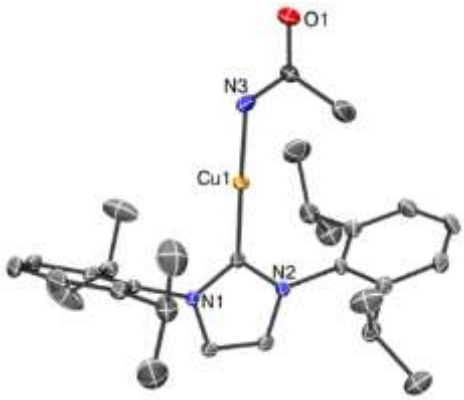

Figure 3. Molecular structure of [Cu(N(H)C(O)CD_3)(IDipp)] (**14**) obtained from single-crystal X-ray diffraction.

X-ray crystallography. Single crystal structures of the free ligand (**1**) and complexes **3-6** and **14** could be refined from single crystal X-ray diffraction data. All atoms could be assigned unambiguously and corroborated the hypothesis of molecular structure (see Figures 3 and 4, and ESI). As expected, the copper containing complexes show coordination to both the carbon and nitrogen atoms of the tfppy ligand, whilst the gold complexes remain linear with only coordination to the acidic C-H group occurring.

Upon closer examination of the coordination geometry of the copper complexes **3** and **4**, and the gold gold complexes **5** and **6**, different surroundings can be observed. In complex **3**, the Cu^{I} center is surrounded by the NHC ligand, the carbon atom C11 of the deprotonated phenyl ring and the nitrogen atom N1 of the pyridyl ring in a trigonal geometry. The C11-Cu1-C12 angle is 160.7(2)°, while the angle between the the NHC, Cu and the nitrogen atom of the pyridyl unit (C12-Cu1-N1) is 118.4(2)°. The angle between both coordinating atoms of the chelating phenylpyridine ligand (C11-Cu1-N1) is with 80.8(2) rather small. Therefore, the coordination of **3** can either be described as distorted trigonal planar or distorted T-shaped. The bond distance between the NHC-carbon atom and the Cu^{I} center in complex **3** (1.899(4) Å) cannot be distinguished from the respective distance in the similar bipyridine complex [Cu(IDipp)(bipy)]BF_4

(1.8919(18) Å),[90] which shows symmetric coordination bond angles between the NHC ligand and the bipyridine ligand with approximately 140° for both. The C11-Cu1 distance (1.969(5) Å) is shorter than the C11-Cu1 distance, which can be attributed to the anionic nature of the deprotonated tetrafluorophenyl ligand. The distance between N1 and Cu1 (2.185(4) Å) is slightly longer than the distances in the bipyridine complex described above (2.061(4) Å and 2.044(2) Å, respectively).[90]

In contrast to the trigonal complex **3**, **4** adopts a distorted tetrahedral geometry with the central Cu^{I} center being surrounded by both phosphorous atoms of the chelating (POP) ligand, the carbon atom C1 of the deprotonated phenyl ring and the nitrogen atom N1 of the pyridyl unit. The angles differ strongly (from 82.27(13)° for C1-Cu1-N1 to 122.85(10)° for C1-Cu1-P1) from ideal tetrahedral geometry. While the distance between the Cu^{I} center and the carbon atom of the deprotonated phenyl ring(Cu1-C1 2.006(3) Å) is slightly longer in **4** than the respective distance in complex **3**, the bond length between Cu1 and N1 (2.135(3) Å) is slightly shorter. Comparison of the Cu1-N1 distance in **4** with the Cu-N distances in [Cu(POP)(bipy)]PF_6[91] (2.0480(16) Å and 2.0738(16) Å, respectively) reveals a longer distance in **4**.

The gold complexes **5** and **6** on the other hand, do not show any coordination of the nitrogen atom. They adopt an almost ideal linear geometry (177.02(10)° in **5** and 177.48(15)° in **6, resp.**) with coordination only to the deprotonated carbon atom of the phenyl ring and either the NHC (complex **5**) or the phosphane (complex **6**).

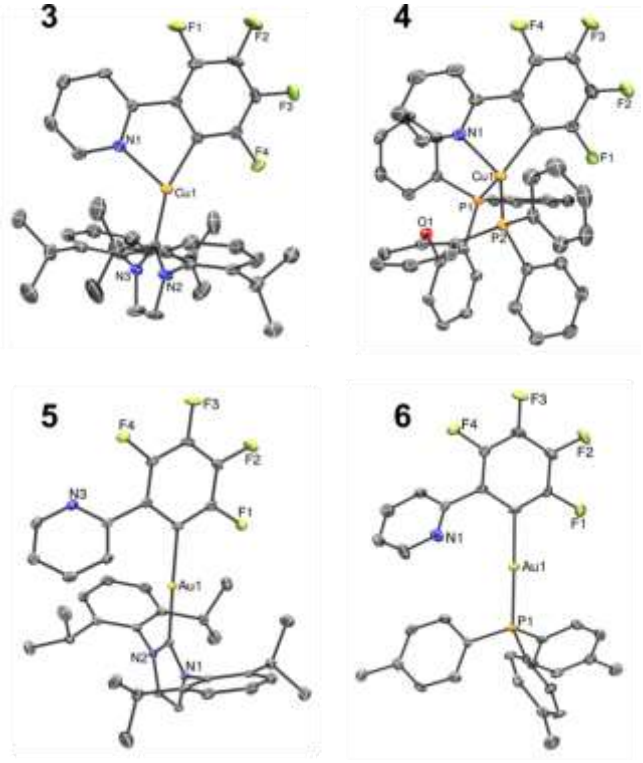

Figure 4. Molecular structures obtained from single-crystal X-ray diffraction of [Cu(tfppy)(IDipp)] (**3**), [Cu(tfppy)(POP)] (**4**), [Au(tfppy)(IDipp)] (**5**) and [Au(tfppy)($PTol_3$)] (**6**).

Absorption and luminescence studies. Important photophysical properties of compounds **3-6** are summarized in Table 1. In the following we will show that the structural differences between the copper and gold ppy-type complexes, i.e. a coordinating (**3** and **4**) or non-ccordinating pyridine moiety (**5** and **6**), play an important role for the photophysical properties, and that the Cu^{I} complexes experience more efficient SOC than the Au^{I} compounds.

In diethylether solution, [Cu(tfppy)(IDipp)] (**3**) and [Cu(tfppy)(POP)] (**4**) show weak absorption bands at 330 and 370 nm, respectively, and at higher energy of 266 (**3**) and 287 (**4**) nm more intense bands with shoulders (Figure 5). The weak emission of **3** is dominated by residual fluorescence at 436 nm with a lifetime of τ = 4.6 ns originating from the coordinated tfppy ligand, due to inefficient intersystem-crossing (ISC) $S_1 \rightarrow T_n$ and radiative decay from the remaining singlet excited states. Coordination of the 2-(tetrafluorophenyl)pyridine ligand to the Cu(I) center leads to a bathochromic shift of the fluorescence, which occurs for the free ligand **1** with a maximum at 352 nm in diethylether solution (Figure 6).

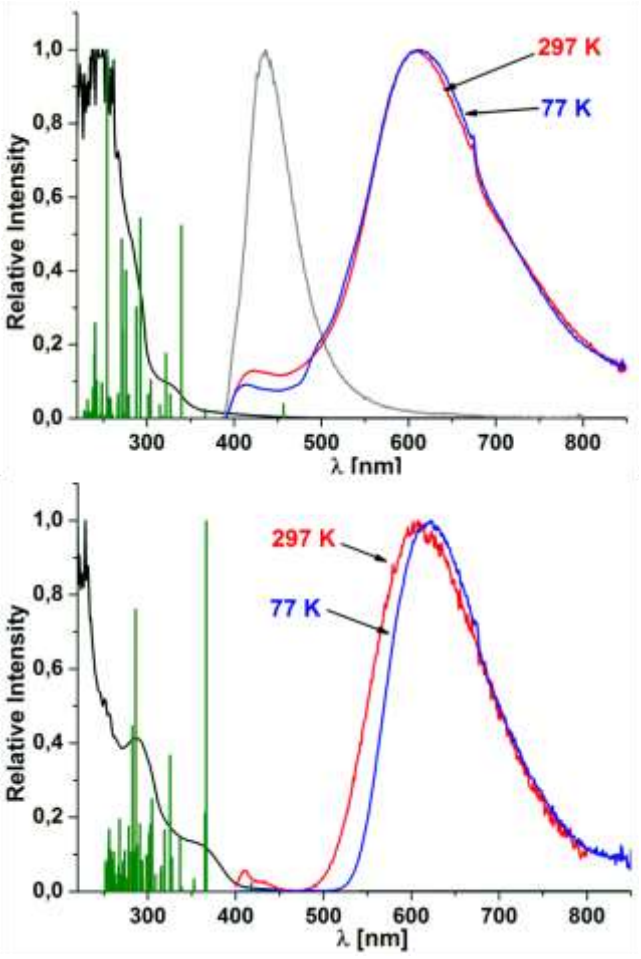

Figure 5. Experimental absorption in solution (Et_2O, black), calculated oscillator strengths (green bars) and emission spectra in Et_2O (grey) and in the solid state (297 K: red, 77 K: blue) of **3** (top) and **4** (bottom).

Table 1. Photophysical Data of 3-6 Obtained in Diethylether Solution, Solid State and PMMA Under Argon.

Cpd.	Solution at 297 K			Solid state at 297 K			Solid state at 77 K		10% in PMMA at 297 K	
	λ_{abs} [nm]	λ_{em} [nm]	τ [ns]	λ_{em} [nm]	$\tau^{a)}$ [µs]	Φ	λ_{em} [nm]	$\tau^{a)}$ [µs]	λ_{em} [nm]	$\tau^{a)}$ [µs]
3	330	436	4.6	610	8.6	0.04	610	21	536	6.4
4	370	-	-	607	9.5	0.06	622	44	615	7.5
5	272	352, 395	- [b)]	370, 472	< 1.0	- [b)]	472	169	448	24
6	270	346, 501	- [b)]	498	17	- [b)]	466	59	501	7.2

a) Amplitude-weighted lifetimes are reported. b) Intensity too weak to be determined.

However, in the solid state the emission becomes much more intense, with the respective maxima at 610 nm for **3**, and at 607 nm for **4**. Due to the fact that the absorption and emission spectra of **3** and **10** are broad and unstructured, they must contain significant charge-transfer (CT) character. The quantum yields of Φ = 0.04 (**3**) and 0.06 (**4**) in conjunction with the luminescence lifetimes τ_{av} = 8.6 (**3**) and 9.5 (**4**) µs are indicative for phosphorescence from a triplet excited state. A comparison with the emission spectra of free Htfppy (**1**) in the solid state and in 2-methyltetrahydrofuran at 77 K, where only fluorescence in the UV region is observable (Figure 6), clearly shows that the phosphorescence in **3** and **4** has to be attributed to the heavy atom effect originating from strong SOC of the copper atom.

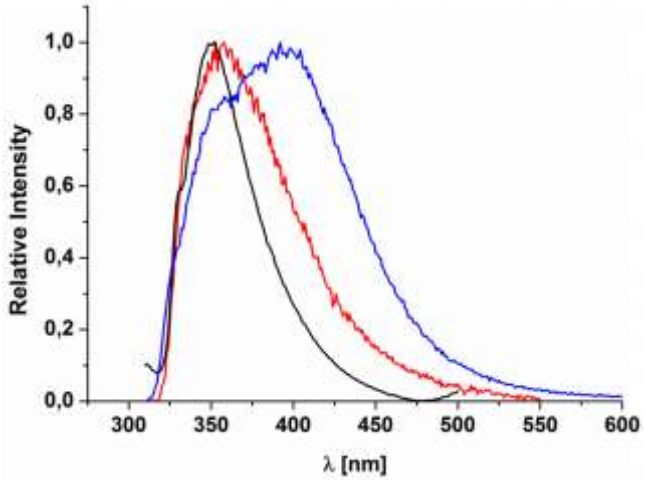

Figure 6. Emission spectra of free Htfppy (**1**) in Et_2O solution (black) and in the solid state (red) at room temperature, and in 2-MeTHF at 77 K (blue).

A good number of Cu^I complexes have been reported in the last few years with short radiative lifetimes of only a few µs due to TADF, which is thermal back-intersystem crossing $T_1 \rightarrow S_1$ and subsequent spin-allowed emission from the singlet state S_1.[24-42,92] At lower temperatures, such systems usually exhibit very long lifetimes of several 10´s to 100´s of µs, because the emission then only occurs from the T_1 state. At 77 K, only [Cu(tfppy)(POP)] (**4**) shows a small shift of the emission maximum to 622 nm, but the lifetimes of both **3** and **4** increase only to an extent, which one would expect for decreased non-radiative decay and not for emission originating from a multiple excited state model. Thus, we assign the Cu^I complexes **3** and **4** as being pure triplet state emitters. It should be mentioned that the linear coordinated Cu^I complex [Cu(3-dfppy)(IDipp)] (**8**) is not luminescent at room temperature.

The absorption spectra of the gold complexes [Au(tfppy)(IDipp)] (**5**) and [Au(tfppy)($PTol_3$)] (**6**) in diethylether are different compared to those of the Cu^I compounds **3** and **4**, as the low energy bands are absent and only intense bands at ca. 250 nm with shoulders at 270 nm are observed (Figure 7). This indicates that the low energy absorptions of the copper(I) tfppy complexes are due to MLCT or ILCT with MLCT admixture, involving the pyridine moiety, which is not possible in the case of the gold(I) tfppy compounds, as those are linearly coordinated with no interaction between the gold atom and the pyridine ring.

5 and **6** are very weakly fluorescent in solution, showing emission maxima in the range of ca. 350-400 nm, which is apparently due to the missing pyridine coordination very similar to the free ligand **1** (λ_{max} = 352 nm) (Figures 6 and 7). However, **6** also exhibits a low energy band centered at 500 nm, which we assign to phosphorescence. This is supported by room temperature solid state emission measurements of the gold phosphine compound **6**, giving only a single broad, very weak emission band at 498 nm with a long lifetime of 17 µs and a very low quantum yield of Φ < 0.01. At 77 K, the phosphorescence intensity increases, and so does the lifetime to 59 µs. In contrast, the Au^I NHC complex **5** shows dual emission also in the solid state at room temperature with maxima at 370 and 472 nm, of which the intensity was too low for reliable lifetime determination. However, comparison with the 77 K emission spectrum and the lifetime of 169 µs allows us to assign the low energy band to be phosphorescence from the T_1 state (Figure 7 and Table 1). Such dual emissive behavior due to inefficient SOC from the gold atom has also been found for gold(I) and gold(III) complexes bearing derivatives of phenanthroline and naphthyl as ligands.[93-95]

However, the linear coordination environment of the Au atom with the missing pyridine coordination in **5** and **6** leads to two effects compared to the Cu^I compounds **3**

and **4**: 1) high energy shift of the phosphorescence and 2) decreased SOC leading to significant additional fluorescence for **5** and very weak phosphorescence for **6**. The first phenomenon is most likely a result of decreased ligand conjugation in the emissive excited state of the gold compounds compared to the copper tfppy complexes, while the second finding originates from a decreased M(d) orbital overlap with the π(py) orbitals (see DFT studies below).

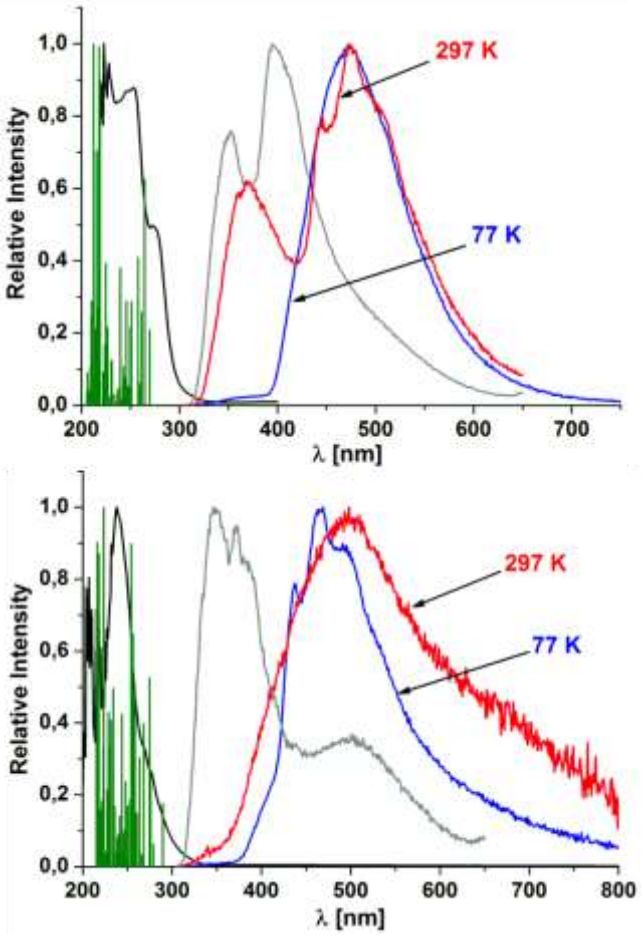

Figure 7. Experimental absorption in solution (Et_2O, solid black), calculated oscillator strengths (red bars) and emission spectra in Et_2O (dashed black) and in the solid state (297 K: dashed red, 77 K: dashed blue) of **5** (top) and **6** (bottom).

We have also prepared PMMA films containing 10% of **3**-**6**, respectively, and recorded their emission spectra and lifetimes. Whereas the emission spectra of **4**-**6** coincide with their solid state luminescence spectra, including the dual emission of **5**, films of [Cu(tfppy)(IDipp)] (**3**) undergo a significant hypsochromic shift of ca. 70 nm (Figure 8). The phosphorescence lifetimes of the copper complexes **3** and **4** in PMMA films are very similar to the solid state (Table 1). However, the gold NHC compound **5** shows an enormous increase in lifetime to 24 μs, and the gold phosphine complex **6** exhibits a decrease to 7.2 μs.

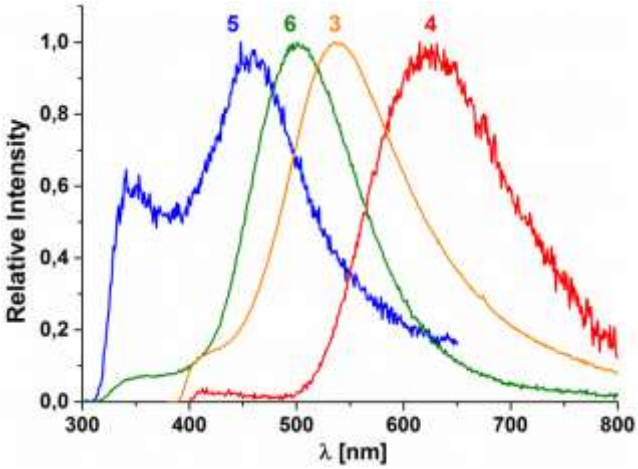

Figure 8. Emission spectra of PMMA films containing 10% of [Cu(tfppy)(IDipp)] (**3**) (red), [Cu(tfppy)(POP)] (**4**) (orange), [Au(tfppy)(IDipp)] (**5**) (blue) and [Au(tfppy)($PTol_3$)] (**6**) (green), respectively, at room temperature.

DFT and TD-DFT studies. In order to gain more insight into the nature of the transitions and emissive excited states of the compounds investigated above, we carried out DFT and TD-DFT calculations at the PBE0/def2-TZVP level of theory. The S_0 ground state structures for the Cu^I complexes **3** and **4**, and the Au^I compounds **5** and **6** agree well with the geometries obtained from single-crystal X-ray diffraction studies. Selected important frontier orbitals of [Cu(tfppy)(IDipp)] (**3**) and [Cu(tfppy)(POP)] (**4**) are depicted in Figure 9, and those of **5** and **6** are given in the ESI. While the frontier orbitals of the free ligand are evenly distributed over the 2,3,4,5-tetrafluorophenyl ring and the pyridine ring (Figure S39), coordination to copper(I) in [Cu(tfppy)(IDipp)] (**3**) and [Cu(tfppy)(POP)] (**4**) leads to more localization of the LUMO at the pyridine moiety. The HOMO in both cases is σ*(M-L) in character, while HOMO-1 becomes a combination of the M(d) and π orbitals of the fluoroarene. HOMO-3 is basically the former HOMO of the free ligand **1**, only that it is more localized at the phenyl moiety.

The simulated absorption spectra obtained from the TD-DFT calculations coincide nicely with the experimental data, and they also display the subtle differences between **3**-**6** (Figures 5 and 7, and ESI). The band between 300-350 nm in the experimental absorption spectrum of [Cu(tfppy)(IDipp)] (**3**) seems to be a mixture of two different types of CTs, one being an M(d)→NHC(π*) MLCT transition ($S_0 \rightarrow S_3$) and the other is of IL(tfppy) nature with some M(d)-tfppy(π*) MLCT admixture ($S_0 \rightarrow S_6$) (Table 2). Interestingly, the fact that the plane of the IDipp ligand is perpendicular to the tfppy ligand allows the HOMO in **3** to interact with the NHC(π*) orbital, while a transition to the ppy-type ligand is symmetry forbidden. The low-energy absorption band between 350-400 nm of [Cu(tfppy)(POP)] (**4**) is a ML(tfppy)CT.

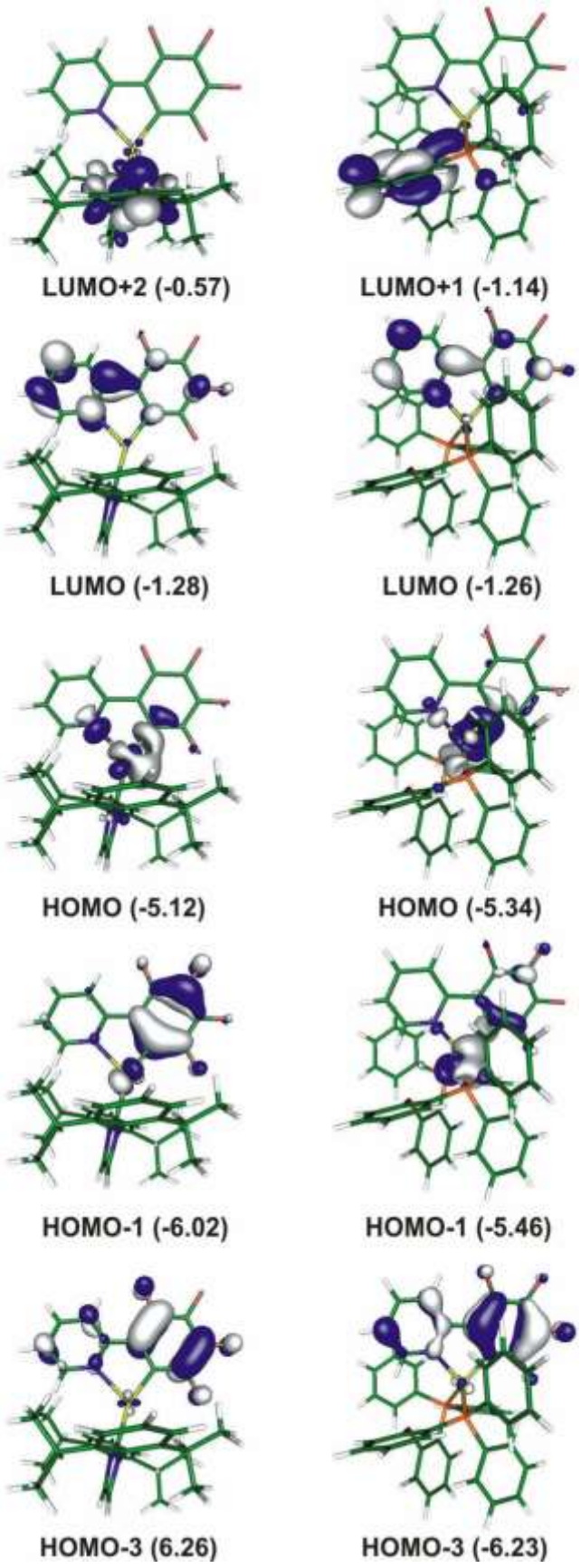

Figure 9. Selected frontier orbitals of [Cu(tfppy)(IDipp)] (**3**) (left) and [Cu(tfppy)(POP)] (**4**) (right). The respective energies in eV are given in brackets.

In stark contrast to **3** and **10**, the missing coordination of the pyridine ring of the tfppy ligand to Au^{I} in [Au(tfppy)(IDipp)] (**5**) and [Au(tfppy)($PTol_3$)] (**6**) leads to localization of the LUMO at the NHC or phosphine ligand *trans* to the fluoroarene, while the HOMO and HOMO-1 are combinations of M(d) and fluoroarene(π) orbitals (Figures S43 and S46). Consequently, the lowest absorption bands of **5** and **6** can be described as *inter*-ligand (tfppy→NHC/$PTol_3$) charge transfer with minor MLCT contributions.

Table 2. Selected results of the TD-DFT calculations for 3-6 obtained at the PBE0/def2-TZVP level.

Cpd.	State	Energy		f	Transition (%)
		[nm]	[eV]		
3	S_1	457	2.72	0.006	H→L (99)
	S_3	340	3.65	0.078	H→L+2 (51)
					H→L+3 (22)
					H→L+6 (10)
	S_6	322	3.85	0.026	H-1→L (48)
					H-2→L (44)
	S_{11}	293	4.24	0.081	H-3→L (48)
					H-5→L (35)
4	S_1	418	2.97	0.003	H→L (83)
					H-1→L (13)
	S_2	367	3.38	0.122	H-1→L (83)
					H→L (13)
	S_8	337	3.68	0.018	H-1→L+2 (60)
					H→L+3 (25)
	S_{24}	286	4.34	0.093	H-3→L (53)
					H→L+10 (12)
5	S_1	269	4.60	0.019	H→L (62)
					H→L+1 (23)
	S_2	264	4.69	0.059	H-1→L (49)
					H-2→L (13)
6	S_1	290	4.28	0.018	H→L+2 (32)
					H→L (27)
					H-2→L+2 (18)
	S_4	275	4.52	0.055	H-1→L+2 (35)
					H-1→L (26)
					H→L+1 (13)
					H-2→L+1 (12)
	S_8	264	4.71	0.032	H-1→L (28)
					H-1→L+1 (24)
					H→L+5 (17)
	S_{13}	254	4.88	0.093	H-3→L+1 (54)

We have optimized the lowest triplet excited states of **3**-**6**, which reveal that the phosphorescence is due to an ^{3}IL(tfppy) state with very little metal(d) participation (Figures 10, S41, S44 and S47), assuming that emission occurs mainly from electron density redistribution between the HSOMO to the LSOMO. The electron is mainly located at the pyridine ring, while the phenyl moiety contains most of the hole. The reason for the emission of the Cu^I complexes being lower in energy compared to the gold compounds presumably lies in the better ligand conjugation due to the coordination of the pyridine to the copper. Furthermore, M(d) orbital interaction with the π electron density should in that case also be more efficient and consequently lead to higher effective SOC from the metal center, and thus to higher quantum yields. It can be assumed that this is why the linear complex [Cu(3-dfppy)(IDipp)] (**8**) shows no significant emission even in the solid state. Also, the missing interaction of the gold atom with the pyridine ring in the triplet state of **5** apparently reduces the effective SOC of the heavy atom, explaining the found residual fluorescence and weak phosphorescence. For **6**, the triplet state shows very weak coordination of the pyridine to Au^I, as the linear arrangement of the NHC ligand and the phenyl ring is unperturbed. However, it should be mentioned that in this case the gas-phase optimization helps to understand the solution behavior of **6**, but it can be assumed that in the solid state a geometry similar to the ground state is maintained, leading to similarly inefficient emission as found for **5**.

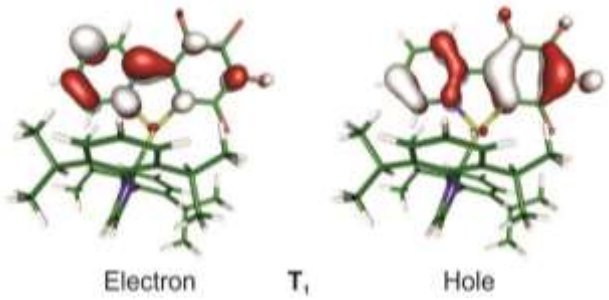

Figure 10. Electron (left) and hole (right) of the optimized triplet excited state T_1 of [Cu(tfppy)(IDipp)] (**3**).

III. CONCLUSIONS

We have reported on the development of a synthetic route to access hitherto unknown Cu^I and Au^I ppy-type complexes, which are luminescent. Coordination of 2-(2,3,4,5-tetrafluorophenyl)pyridine (**1**) to Cu^I has been achieved either via C-H activation using [Cu(OH)(IDipp)] (**2**) in THF, or by lithiation and subsequent reaction with $CuBr{\cdot}SMe_2$ in the presence of POP, giving the two copper complexes [Cu(tfppy)(IDipp)] (**3**) and [Cu(tfppy)(POP)] (**4**), respectively. The C-H activation pathway carried out in acetonitrile results in an unusual Cu^I mediated hydroxylation of the solvent, leading to the isolation of a copper(I) acetamide species, i.e. [Cu(NHC(O)Me)(IDipp)] (**14**). Interestingly, employing 2-(2,4-difluorophenyl)-pyridine (**7**) as a ligand, Cu-C bond formation is only observed in the 3-position of the phenyl ring, giving the linear coordinated, non-luminescent Cu^I aryl complex **8**. In contrast to trigonal **3** and tetrahedral **4**, the corresponding NHC and phosphine Au^I tfppy compounds, [Au(tfppy)(IDipp)] (**5**) and [Au(tfppy)($PTol_3$)] (**6**), show linear coordination geometries around the coinage metal center, with the nitrogen of tfppy not binding to Au^I.

The coordination of the pyridine moiety of the ppy-type ligands has a profound effect on the luminescence properties of the Cu^I and Au^I complexes. The copper compound **3** is weakly emissive in solution, but like **4** it is intensely luminescent in the solid state, exhibiting orange-red phosphorescence from an ^{3}IL state at room temperature. In contrast, the linear Au^I complexes **5** and **6** are very weakly phosphorescent even in the solid state due to insufficient SOC, with **5** showing additional fluorescence at 297 K. Also, the linear complex [Cu(3-dfppy)(IDipp)] (**8**) shows no emission at room temperature in the solid state.

Our current efforts are devoted to optimizing the emission properties of coinage metal ppy-type complexes by chemical modification, which includes tuning of the emission color and the luminescence efficiency.

IV. EXPERIMENTAL DETAILS

General Conditions. Htfppy (**1**) was synthesized following a literature known procedure.[84] All other starting materials were purchased from commercial sources and were used without further purification. The organic solvents for synthetic reactions and for photophysical and were HPLC grade, further treated to remove trace water using an Innovative Technology Inc. Pure-Solv Solvent Purification System and deoxygenated by purging with Argon. All synthetic reactions were performed in an Innovative Technology Inc. glovebox or under an argon atmosphere using standard Schlenk techniques. ^{1}H, ^{13}C{^{1}H}, ^{13}C{^{19}F}, ^{19}F, ^{31}P, (^{15}N, ^{1}H) HMBC NMR spectra were measured either on a Bruker Avance 500 (^{1}H, 500 MHz; ^{13}C, 125 MHz; ^{19}F, 470 MHz; ^{31}P 202 MHz) or on a Bruker Advance 200 (^{1}H, 200 MHz; ^{7}Li, 77 MHz; ^{19}F, 188 MHz) NMR spectrometer. The MALDI mass spectra above were performed with a Bruker Daltonics autoflex II mass spectrometer, equipped with a MidiNitrogen laser MNL (LTB Lasertechnik, Berlin) operating at 337 nm. Calibration was performed externally with 1 µl of a mixture of 10 mg/ml PEG1000 (Lancaster) in methanol, a saturated solution of 2,5-dihydroxybenzoic acid (Bruker Daltonics) in methanol and sodium iodide (1 mg/ml in Methanol) in a ratio of 10:10:1. 1 µl of the sample solution (2 mM in THF) and 2 µl of a 100 mg/ml matrix solution (2-[(2E)-3-(4-*tert*-butylphenyl)-2-methylprop-2-enylidene]malononitrile (DCTB; Fluka)) in THF were mixed and 0,5–1 µl were dropped onto the stainless steel target (MTP 384 massive target T; Bruker Daltonics

#26755). Due to the isotopic distribution over a broad m/z region caused by chlorine, and/or bromine the signal of monoisotopic signals was too small for some compounds in intensity for an accurate mass measurement. In this case, typically the most intense signal (X+n) of this isotopic distribution was taken as described and compared with the respective calculated value. For calculation of the respective mass values of the isotopic distribution, the software modul "Bruker Daltonics IsotopePattern" of the software Compass 1.1 from Bruker Daltonik GmbH, Bremen was used.

Photophysical measurements. All experiments were carried out on crystalline samples, of which the respective unit cell was determined for several crystals of the bulk sample before the measurements in order to exclude impurities. Furthermore, multiple trials of the same experiment/data collection ensured reproducibility. UV-visible absorption spectra were obtained on an Agilent 1100 Series Diode Array spectrophotometer using standard 1 cm path length quartz cells. Excitation and emission spectra were recorded on an Edinburgh Instrument FLSP920 spectrometer, equipped with a 450 W Xenon arc lamp, double monochromators for the excitation and emission pathways, and a red-sensitive photomultiplier (PMT-R928) as detector. The excitation and emission spectra were corrected using the standard corrections supplied by the manufacturer for the spectral power of the excitation source and the sensitivity of the detector. The quantum yields were measured by use of an integrating sphere with an Edinburgh Instrument FLSP920 spectrometer. The luminescence lifetimes were measured using a µF900 pulsed 60 W Xenon microsecond flashlamp, with a repetition rate of 100 Hz, and a multichannel scaling module. The emission was collected at right angles to the excitation source with the emission wavelength selected using a double grated monochromator and detected by a R928-P PMT. Low temperature measurements were performed in an Oxford Optistat cryostat.

X-ray Crystallography. Crystals suitable for single-crystal X-ray diffraction were selected, coated in perfluoropolyether oil, and mounted on MiTeGen sample holders. Diffraction data were collected on a Nonius Kappa three circle diffractometer utilizing graphite monochromated MoKα radiation (λ = 0.71073 Å) from a rotating anode tube run at 50 V and 30 mA. The diffractometer is equipped with a Bruker ApexII area detector and an open flow N2 Cryoflex II (Bruker) device, the measurement was performed at 100 K. For data reduction, the Bruker Apex2 software suite (Bruker AXS) was used. Subsequently, utilizing Olex2[96] or ShelX[97] the structures were solved using the Olex2.solve[98] charge-flipping algorithm or ShelXT[99], and were subsequently refined with Olex2.refine[98] using Gauss-Newton minimization or ShelXle. All non-hydrogen atom positions were located from the Fourier maps and refined anisotropically. Hydrogen atom positions were calculated using a riding model in geometric positions and refined isotropically, where possible to determine unambiguously.

Computational Details. Calculations (gas-phase) were performed with the ORCA 3.0.2 program suite.[100] Geometry optimizations were carried out either with the PBE0[101-107] functional, or with the BP86[108-109] functional, followed by a single point calculation with PBE0, as implemented in ORCA, and a frequency analysis ensuring that the optimized structures correspond to global energy minima. The def2-TZVP[110-111] basis set was used for all atoms together with the auxiliary basis set def2-TZVP/J in order to accelerate the computations within the framework of RI approximation. Relativistic effects of the Cu(I) complexes were accounted for by employing the ZORA[112] method, while for Au(I) an ECP of def2-tvzp quality has been employed,[111,113,114] and van der Waals interactions have been considered by an empirical dispersion correction (Grimme-D3BJ).[115,116] TD-DFT calculations for the first 50 singlet and triplet excited states were performed with the same functional. Representations of molecular orbitals were produced with orca_plot as provided by ORCA 3.0.2 and with gOpenMol 3.00.[117,118]

Synthesis. *[Cu(tfppy)(IDipp)] (**3**).* [Cu(OH)(IPr)] (**2**) (469 mg, 1 mmol) was dissolved in THF (10 ml) in a scintillation vial and 200 mg molecular sieves (4 Å) and **1** (228 mg, 1 mmol) were added. The reaction mixture was stirred at -30°C for 24 hours, then filtered over celite and the volatiles were evaporated under reduced pressure to give a red powder. The solid was dissolved in the smallest amount of THF possible, layered with diethylether and stored for 2 days at -30°C to give **3** as red crystals (437 mg, 63%). ^{1}H NMR (d^{8}-THF, 500 MHz): δ 7.90 (m, 1H), 7.76 (m, 1H), 7.53 (m, 2H), 7.45 (s, 2H), 7.37 (m, 4H), 7.00 (m, 1H), 6.83 (m, 1H), 2.90 (hept, 4H), 1.29 (d, J_{HH} = 6.79 Hz, 12H), 1.22 (d, J_{HH} = 6.79 Hz, 12H) ppm. ^{13}C{^{1}H} NMR (d^{8}-THF, 125 MHz): δ185.8 (s), 156.43 (bs), 148.7 (s), 148.4 (m), 145.9 (m), 145.7 (s), 139.0 (m), 136.9 (m), 136.4 (s), 129.6 (s), 123.93 (s), 123.3 (s), 123.03 (s), 122.6 (s), 120.9 (s), 28.2 (s), 23.7 (s), 23.3 (s) ppm. ^{13}C{^{19}F} NMR (d^{8}-THF, 125 MHz): δ185.8 (s), 156.43 (bs), 148.7 (ddd, J_{CH} = 181, 7, 2 Hz), 148.4 (s), 145.9 (s), 145.7 (bs), 139.0 (s), 136.9 (s), 136.4 (bs), 129.6 (m, J_{CH} = 159 Hz), 123.93 (ddd, J_{CH} = 159, 7, 4 Hz), 123.9 (bs), 123.3 (dd, J_{CH} = 196, 13 Hz), 123.03 (m), 122.6 (m, J_{CH} = 141, 12 Hz), 120.9 (ddd, J_{CH} = 162, 9, 6 Hz), 28.2 (m, J_{CH} = 126 Hz), 23.7 (m), 23.3 (m) ppm. ^{19}F NMR (d^{8}-THF, 470 MHz): δ-105.87 (m), -143.3 (m), -157.2 (m), -165.1 (m) ppm. ^{15}N NMR (d^{8}-THF, 51 MHz): δ-185.9 (s, N_{NHC}), -85.7 (s, N_{py}) ppm. MALDI/TOF: m/z 930 (M+DCTB+H) $^{+}$. Anal. Calcd for $CuC_{47}H_{32}NF_4P_2O$: C, 67.29; H, 5.94; N, 6.21. Found: C, 66.82; H, 5.61; N, 6.68.

*General Procedure for the Preparation of **4**-**6**.* **1** and 2 equiv of freshly distilled TMEDA were dissolved in THF (10 ml) and cooled to -40°C. Then, 1.2 equiv *n*BuLi (1.6M in THF) was added and the solution stirred for 4 hours. The tfppyLi·TMEDA solution was transferred via cannula to a cooled suspension of the respective metal halide complex and ligand in THF (10 ml) at -40°C. After stirring for 4 hours at -40°C, the mixture was allowed to warm to room

temperature overnight. The volatiles were removed *in vacuo* and the resulting powder was extracted with an appropriate solvent.

*[Cu(tfppy)(POP)] (**4**).* **4** was generated from **1** (228 mg, 1 mmol), CuBr (143 mg, 1 mmol) and POP ligand (538 mg, 1 mmol). After extraction with a 2:1 mixture of hexane/THF (3 · 20 ml) and evaporation of the volatiles, **4** was obtained as yellow powder (320 mg, 38%). Crystals suitable for X-Ray diffraction were obtained by layering a saturated solution of THF with diethylether at -30°C. ^{1}H NMR (C_6D_6, 500 MHz): δ 8.19 (m, J_{HH} = 9 Hz, 1H), 8.10 (m, J_{HH} = 4 Hz, 1H), 8.08-7.56 (br, 4H), 7.12-6.61 (br, 24H), 6.49 (m, 2H), 6.13 (ddd, J_{HH} = 7, 5, 1 Hz, 1H) ppm. ^{13}C{^{1}H} NMR (C_6D_6, 125 MHz): δ 159.0 (vt), 157.3 (bs), 149.1 (s), 136.2 (s), 135.0 (bs), 134.8 (s), 132.5 (bs), 130.4 (s), 126.7 (vt), 124.3 (s), 123.4 (d, J_{CP} = 19 Hz), 120.6 (s), 120.2 (s) ppm. ^{13}C{^{19}F} NMR (C_6D_6, 125 MHz): δ 160.2 (vt), 159.0 (m), 157.3 (m), 149.0 (ddd, J_{CH} = 180, 7, 4 Hz), 148.6 (s), 148.0 (s), 139.9 (s), 136.8 (s), 136.2 (dd, J_{CH} = 162, 7 Hz), 135.0 (bd, J_{CH} = 160 Hz), 134.8 (ddd, J_{CH} = 162, 8, 2 Hz), 132.5 (bd, J_{CH} = 160 Hz), 130.4 (ddd, J_{CH} = 162, 8, 2 Hz), 128.6 (s, C_{ipso}), 126.7 (m), 125.1 (s), 124.3 (dd, J_{CH} = 161, 8 Hz), 123.4 (d, J_{CH} = 166 Hz, J_{CP} = 19 Hz), 120.6 (m, J_{CH} = 164, 7 Hz), 120.2 (d, J_{CH} = 162, 9 Hz) ppm. ^{19}F NMR (C_6D_6, 470 MHz): δ -105.2 (m), -138.9 (m), -153.9 (m), -163.6 (m) ppm. ^{31}P NMR (C_6D_6, 202 MHz): δ -10.4 (s) ppm. ^{15}N NMR (C_6D_6, 470 MHz): δ -100.8 (s) ppm. MALDI/TOF: m/z 827.1 $(M+H)^+$, 601 $(Cu+POP)^+$. Anal. Calcd for $CuC_{47}H_{32}NF_4P_2O$: C, 68.16; H, 3.89; N, 1.69. Found: C, 67.72; H, 3.73; N, 1.51.

*[Au(tfppy)(IDipp)] (**5**).* **5** was obtained from **1** (228 mg, 1 mmol) and [AuCl(IDipp)] (620 mg, 1 mmol). Extraction was carried out with dichloromethane (3 · 10ml). After concentration and layering with hexane, white crystals of **5** formed at -30°C (540 mg, 65%). ^{1}H NMR (C_6D_6, 500 MHz): δ 8.23 (m, J_{HH} = 5 Hz, 1 Hz, 1H), 7.33 (m, 2H), 7.13 (m, J_{HH} = 8 Hz, 1H), 7.03 (m, 4H), 6.84 (m, J_{HH} = 8 Hz, 2 Hz, 1H), 6.59 (m, 1H), 6.25 (s, 2H), 2.50 (heptet, J_{HH} = 7 Hz, 4H) , 1.26 (d, J_{HH} = 7 Hz, 12H), 1.04 (d, J_{HH} = 7 Hz, 12H) ppm. ^{13}C{^{1}H} NMR (C_6D_6, 125 MHz): δ 193.4 (s), 159.1 (br), 150.1 (m, J_{CF} = 222 Hz), 149.9 (m, J_{CF} = 56 Hz, C_{ipso}), 148.3 (s), 146.1 (m, J_{CF} = 250 Hz, 11 Hz, 3 Hz), 145.4 (s), 140.0 (m, J_{CF} = 256 Hz, 27 Hz, 13 Hz), 138.0 (m, J_{CF} = 244 Hz), 134.5 (s), 134.5 (s), 131.9 (m, J_{CF} = 20 Hz, 6, 5 Hz), 130.3 (s), 124.5 (br), 123.9 (s), 122.5 (s), 120.7 (s), 28.6 (s), 24.2 (s), 23.5 (s) ppm. ^{13}C{^{19}F} NMR (C_6D_6, 125 MHz): δ 193.4 (s), 159.1 (m, J_{CH} = 11 Hz, 7 Hz), 150.1 (s), 149.9 (s), 148.3 (ddd, J_{CH} = 177 Hz, 7 Hz, 3 Hz), 146.1 (s), 145.4 (m), 140.0 (s), 138.0 (s), 134.5 (dd, J_{CH} = 161 Hz, 7 Hz), 134.5 (m), 131.9 (s), 130.3 (d, J_{CH} = 160 Hz), 124.5 (dd, J_{CH} = 161 Hz, 7 Hz), 123.9 (dm, J_{CH} = 158 Hz), 122.5 (dd, J_{CH} = 197 Hz, 11 Hz, 3 Hz), 120.7 (dm, J_{CH} = 162 Hz, 6 Hz), 28.6 (dm, J_{CH} = 130 Hz), 24.2 (qm, J_{CH} = 125 Hz), 23.5 (qm, J_{CH} = 125 Hz) ppm. ^{19}F NMR (C_6D_6, 470 MHz): δ -115.6 (m), -143.8 (m), -158.7 (m), -162.7 (m) ppm. MALDI/TOF: m/z 811 $(M+H)^+$, 1060 $(M+DCTB)^+$. Anal. Calcd for $AuC_{38}H_{38}N_3F_4$: C, 56.23; H, 4.97; N, 5.18. Found: C, 55.75; H, 4.95; N, 5.30.

*[Au(tfppy)($PTol_3$)] (**6**).* **6** was obtained from **1** (228 mg, 1 mmol), AuCl·SMe_2 (294 mg, 1 mmol) and $PTol_3$ (304 mg, 1 mmol). Extraction was carried out with dichloromethane (3 · 10ml). The organic phase was concentrated, layered with hexane and stored at -30°C giving **6** as white crystals (420 mg, 57%). ^{1}H NMR (C_6D_6, 500 MHz): δ 8.45 (dm, J_{HH} = 5 Hz, 2, 1 Hz, 1H), 7.54 (m, J_{HH} = 8 Hz, 1H), 7.39 (m, 6H), 7.07 (m, 1H), 6.83 (m, 1H), 6.63 (m, 1H), 1.95 (s, 9H) ppm. ^{13}C{^{1}H} NMR (C_6D_6, 125 MHz): δ 158.1 (m), 154.9 (m, J_{CF} = 60 Hz, C_{ipso}), 150.0 (m, J_{CF} = 217 Hz, CF), 149.2 (s), 146.9 (m, J_{CF} = 251 Hz, CF), 141.1 (d, J_{CF} = 3 Hz), 140.8 (m, J_{CF} = 259 Hz), 138.8 (m, J_{CF} = 225 Hz), 135.1 (s), 134.1 (d, J_{CP} = 15 Hz), 129.6 (d, J_{CP} = 11 Hz), 128.4 (d, J_{CP} = 51 Hz), 125.3 (d, J_{CP} = 6 Hz), 121.3 (s), 20.8 (d, J_{CP} = 2 Hz) ppm. ^{13}C{^{19}F} NMR (C_6D_6, 125 MHz): δ 158.1 (m), 154.9 (s), 150.0 (s), 149.2 (ddd, J_{CH} = 178 Hz, 7 Hz, 3 Hz), 146.9 (s), 141.1 (m), 140.7 (s), 138.7 (s), 135.1 (dd, J_{CH} = 162 Hz, 6 Hz), 134.1 (dd, J_{CH} = 168 Hz, 7 Hz, J_{CP} = 15Hz), 129.6 (dm, J_{CH} = 160 Hz, J_{CP} = 11 Hz), 128.4 (dm, J_{CH} = 8 Hz, J_{CP} = 51 Hz), 125.3 (dm, J_{CH} = 164 Hz, 2 Hz, J_{CP} = 6 Hz), 121.3 (dm, J_{CH} = 162 Hz, 7 Hz), 20.8 (qm, J_{CH} = 126 Hz, 4 Hz, J_{CP} = 2 Hz) ppm. ^{19}F NMR (C_6D_6, 470 MHz): δ -112.9 (m), -142.6 (m), -156.5 (m), -160.2 (m) ppm. ^{31}P NMR (C_6D_6, 202 MHz): δ 36.22 ppm. MALDI/TOF: m/z 727.100 $(M+H)^+$. Anal. Calcd for $AuC_{32}H_{25}NF_4P$: C, 52.83; H, 3.46; N, 1.93. Found: C, 52.87; H, 3.42; N, 2.15.

ASSOCIATED CONTENT

Supporting Information. Further details of X-ray crystallography, results of DFT and TD-DFT calculations, as well as NMR spectra of all compounds reported in this work can be found in the Supporting Information. This material is available free of charge via the Internet at http://pubs.acs.org.

AUTHOR INFORMATION

Corresponding Author

* andreas.steffen@uni-wuerzburg.de

Present Address

† School of Medicine, Pharmacy and Health, Durham University, University Boulevard, Stockton-on-Tees, TS17 6BH (UK).

Notes

The authors declare no competing financial interest.

ACKNOWLEDGMENT

We thank the DFG (STE 1834/4-1) for financial support. This work has also been supported by the Collaborative Research Network "Solar Technologies go Hybrid" of the Bavarian State Ministry of Science, Research, and the Arts, which we gratefully acknowledge. We thank Dr. Andreas Lorbach and Mr. Marius Schäfer for help with one X-ray diffraction experiment. AS thanks Prof. Todd B. Marder for his generous support.

REFERENCES

(1) Bomben, P. G.; Robson, K. C. D.; Koivisto, B. D.; Berlinguette, C. P. *Coord. Chem. Rev.* **2012**, *256*, 1438-1450.
(2) Crabtree, R. H. *Organometallics* **2011**, *30*, 17-19.

(3) Chou, P.-T.; Chi, Y.; Chung, M.-W.; Lin, C.-C. *Coord. Chem. Rev.* **2011**, *255*, 2653-2665.
(4) Wong, W.-Y.; Ho, C.-L. *Acc. Chem. Res.* **2010**, *43*, 1246-1256.
(5) Rausch, A. F.; Homeier, H. H. H.; Yersin, H. *Top. Organomet. Chem.* **2010**, *29*, 193-235.
(6) Morris, A. J.; Meyer, G. J.; Fujita, E. *Acc. Chem. Res.* **2009**, *42*, 1983-1994.
(7) Grätzel, M. *Acc. Chem. Res.* **2009**, *42*, 1788-1798.
(8) Yersin, H. *Top. Curr. Chem.* **2004**, *241*, 1-26.
(9) Polo, A. S.; Itokazu, M. K.; Murakami Iha, N. Y. *Coord. Chem. Rev.* **2004**, *248*, 1343-1361.
(10) Grätzel, M. *J. Photochem. Photobiol., C* **2003**, *4*, 145-153.
(11) Arakawa, H.; Aresta, M.; Armor, J. N.; Barteau, M. A.; Beckman, E. J.; Bell, A. T.; Bercaw, J. E.; Creutz, C.; Dinjus, E.; Dixon, D. A.; Domen, K.; DuBois, D. L.; Eckert, J.; Fujita, E.; Gibson, D. H.; Goddard, W. A.; Goodman, D. W.; Keller, J.; Kubas, G. J.; Kung, H. H.; Lyons, J. E.; Manzer, L. E.; Marks, T. J.; Morokuma, K.; Nicholas, K. M.; Periana, R.; Que, L.; Rostrup-Nielson, J.; Sachtler, W. M. H.; Schmidt, L. D.; Sen, A.; Somorjai, G. A.; Stair, P. C.; Stults, B. R.; Tumas, W. *Chem. Rev.* **2001**, *101*, 953-996.
(12) Hagfeldt, A.; Grätzel, M. *Acc. Chem. Res.* **2000**, *33*, 269-277.
(13) Kalyanasundaram, K.; Grätzel, M. *Coord. Chem. Rev.* **1998**, *177*, 347-414.
(14) Flamigni, L.; Barbieri, A.; Sabatini, C.; Ventura, B.; Barigelletti, F. *Top. Curr. Chem.* **2007**, *281*, 143-203.
(15) Campagna, S.; Puntoriero, F.; Nastasi, F.; Bergamini, G.; Balzani, V. *Top. Curr. Chem.* **2007**, *280*, 117-214.
(16) Armaroli, N. *Chem. Soc. Rev.* **2001**, *30*, 113-124.
(17) Armaroli, N.; Accorsi, G.; Cardinali, F.; Listorti, A. *Top. Curr. Chem.* **2007**, *280*, 69-115.
(18) Yersin, H.; Rausch, A. F.; Czerwieniec, R.; Hofbeck, T.; Fischer, T. *Coord. Chem. Rev.* **2011**, *255*, 2622-2652.
(19) Blasse, G.; McMillin, D. R. *Chem. Phys. Lett.* **1980**, *70*, 1-3.
(20) Breddels, P. A.; Berdowski, P. A. M.; Blasse, G.; McMillin, D. R. *J. Chem. Soc., Faraday Trans. 2* **1982**, *78*, 595-601.
(21) Kirchhoff, J. R.; Gamache, R. E., Jr.; Blaskie, M. W.; Del, P. A. A.; Lengel, R. K.; McMillin, D. R. *Inorg. Chem.* **1983**, *22*, 2380-2384.
(22) Everly, R. M.; McMillin, D. R. *J. Phys. Chem.* **1991**, *95*, 9071-9075.
(23) Pallenberg, A. J.; Koenig, K. S.; Barnhart, D. M. *Inorg. Chem.* **1995**, *34*, 2833-2840.
(24) Czerwieniec, R.; Yu, J.-B.; Yersin, H. *Inorg. Chem.* **2011**, *50*, 8293-8301.
(25) Chen, X.-L.; Yu, R.; Zhang, Q.-K.; Zhou, L.-J.; Wu, X.-Y.; Zhang, Q.; Lu, C.-Z. *Chem. Mater.* **2013**, *25*, 3910-3920.
(26) Osawa, M.; Kawata, I.; Ishii, R.; Igawa, S.; Hashimoto, M.; Hoshino, M. *J. Mater. Chem. C* **2013**, *1*, 4375-4383.
(27) Volz, D.; Zink, D. M.; Bocksrocker, T.; Friedrichs, J.; Nieger, M.; Baumann, T.; Lemmer, U.; Bräse, S. *Chem. Mater.* **2013**, *25*, 3414-3426.
(28) Zink, D. M.; Bächle, M.; Baumann, T.; Nieger, M.; Kuhn, M.; Wang, C.; Klopper, W.; Monkowius, U.; Hofbeck, T.; Yersin, H.; Bräse, S. *Inorg. Chem.* **2013**, *52*, 2292-2305.
(29) Zink, D. M.; Baumann, T.; Friedrichs, J.; Nieger, M.; Bräse, S. *Inorg. Chem.* **2013**, *52*, 13509-13520.
(30) Zink, D. M.; Volz, D.; Baumann, T.; Mydlak, M.; Flügge, H.; Friedrichs, J.; Nieger, M.; Bräse, S. *Chem. Mater.* **2013**, *25*, 4471-4486.
(31) Bizzarri, C.; Strabler, C.; Prock, J.; Trettenbrein, B.; Ruggenthaler, M.; Yang, C.-H.; Polo, F.; Iordache, A.; Brüggeller, P.; de Cola, L. *Inorg. Chem.* **2014**, *53*, 10944-10951.
(32) Osawa, M. *Chem. Commun.* **2014**, *50*, 1801-1803.
(33) Osawa, M.; Hoshino, M.; Hashimoto, M.; Kawata, I.; Igawa, S.; Yashima, M. *Dalton Trans.* **2015**, *44*, 8369-8378.
(34) Yersin, H.; Rausch, A. F.; Czerwieniec, R.; Hofbeck, T.; Fischer, T. *Coord. Chem. Rev.* **2011**, *255*, 2622-2652.
(35) Czerwieniec, R.; Kowalski, K.; Yersin, H. *Dalton Trans.* **2013**, *42*, 9826-9830.
(36) Leitl, M. J.; Küchle, F. R.; Mayer, H. A.; Wesemann, L.; Yersin, H. *J. Phys. Chem. A* **2013**, *117*, 11823-11836.
(37) Leitl, M. J.; Krylova, V. A.; Djurovich, P. I.; Thompson, M. E.; Yersin, H. *J. Am. Chem. Soc.* **2014**, *136*, 16032-16038.
(38) Linfoot, C. L.; Leitl, M. J.; Richardson, P.; Rausch, A. F.; Chepelin, O.; White, F. J.; Yersin, H.; Robertson, N. *Inorg. Chem.* **2014**, *53*, 10854-10861.
(39) Czerwieniec, R.; Yersin, H. *Inorg. Chem.* **2015**, *54*, 4322-4327.
(40) Gneuss, T.; Leitl, M. J.; Finger, L. H.; Rau, N.; Yersin, H.; Sundermeyer, J. *Dalton Trans.* **2015**, *44*, 8506-8520.
(41) Hofbeck, T.; Monkowius, U.; Yersin, H. *J. Am. Chem. Soc.* **2015**, *137*, 399-404.
(42) Deaton, J. C.; Switalski, S. C.; Kondakov, D. Y.; Young, R. H.; Pawlik, T. D.; Giesen, D. J.; Harkins, S. B.; Miller, A. J. M.; Mickenberg, S. F.; Peters, J. C. *J. Am. Chem. Soc.* **2010**, *132*, 9499-9508.
(43) Visbal, R.; Gimeno, M. C. *Chem. Soc. Rev.* **2014**, *43*, 3551-3574.
(44) Fortman, G. C.; Slawin, A. M. Z.; Nolan, S. P. *Organometallics* **2010**, *29*, 3966-3972.
(45) Herron, J. R.; Ball, Z. T. *J. Am. Chem. Soc.* **2008**, *130*, 16486-16487.
(46) Do, H. Q.; Daugulis, O. *J. Am. Chem. Soc.* **2008**, *130*, 1128-1129.
(47) Do, H. Q.; Khan, R. M. K.; Daugulis, O. *J. Am. Chem. Soc.* **2008**, *130*, 15185-15192.
(48) Chu, L.; Qing, F.-L. *J. Am. Chem. Soc.* **2012**, *134*, 1298-1304.
(49) Fan, S.; Chen, F.; Zhang, X. *Angew. Chem., Int. Ed.* **2011**, *50*, 5918-5923.
(50) Nakatani, A.; Hirano, K.; Satoh, T.; Miura, M. *Org. Lett.* **2012**, *14*, 2586-2589.
(51) Shang, R.; Fu, Y.; Wang, Y.; Xu, Q.; Yu, H.-Z.; Liu, L. *Angew. Chem., Int. Ed.* **2009**, *48*, 9350-9354.
(52) Leoni, P.; Pasquali, M.; Ghilardi, C. A. *J. Chem. Soc., Chem. Commun.* **1983**, 240-241.
(53) Hope, H.; Olmstead, M. M.; Power, P. P.; Sandell, J.; Xu, X. *J. Am. Chem. Soc.* **1985**, *107*, 4337-4338.
(54) He, X.; Olmstead, M. M.; Power, P. P. *J. Am. Chem. Soc.* **1992**, *114*, 9668-9670.
(55) Schiemenz, B.; Power, P. P. *Organometallics* **1996**, *15*, 958-964.
(56) Hwang, C.-S.; Power, P. P. *Organometallics* **1999**, *18*, 697-700.
(57) Niemeyer, M. *Z. Anorg. Allg. Chem.* **2003**, *629*, 1535-1540.
(58) Niemeyer, M. *Z. Anorg. Allg. Chem.* **2004**, *630*, 252-256.
(59) Sundararaman, A.; Zakharov, L. N.; Rheingold, A. L.; Jäkle, F. *Chem. Commun.* **2005**, 1708-1710.
(60) Ohishi, T.; Nishiura, M.; Hou, Z. *Angew. Chem., Int. Ed.* **2008**, *47*, 5792-5795.
(61) Haywood, J.; Morey, J. V.; Wheatley, A. E. H.; Liu, C.-Y.; Yasuike, S.; Kurita, J.; Uchiyama, M.; Raithby, P. R. *Organometallics* **2009**, *28*, 38-41.
(62) Ito, M.; Hashizume, D.; Fukunaga, T.; Matsuo, T.; Tamao, K. *J. Am. Chem. Soc.* **2009**, *131*, 18024-18025.
(63) Bomparola, R.; Davies, R. P.; Hornauer, S.; White, A. J. P. *Dalton Trans.* **2009**, 1104-1106.
(64) Groysman, S.; Holm, R. H. *Inorg.Chem.* **2009**, *48*, 621-627.
(65) An, D.; Wang, J.; Dong, T.; Yang, Y.; Wen, T.; Zhu, H.; Lu, X.; Wang, Y. *Eur. J. Inorg. Chem.* **2010**, *2010*, 4506-4512.
(66) Bomparola, R.; Davies, R. P.; Lal, S.; White, A. J. P. *Organometallics* **2012**, *31*, 7877-7883.
(67) Bomparola, R.; Davies, R. P.; Hornaeur, S.; White, A. J. P. *Dalton Trans.* **2014**, *43*, 14359-14367.

(68) Ueno, A.; Takimoto, M.; O, W. W. N.; Nishiura, M.; Ikariya, T.; Hou, Z. *Chem. Asian J.* **2015**, *10*, 1010-1016.
(69) Doshi, A.; Sundararaman, A.; Venkatasubbaiah, K.; Zakharov, L. N.; Rheingold, A. L.; Myahkostupov, M.; Piotrowiak, P.; Jäkle, F. *Organometallics* **2012**, *31*, 1546-1558.
(70) Doshi, A.; Venkatasubbaiah, K.; Rheingold, A. L.; Jäkle, F. *Chem. Commun.* **2008**, 4264-4266.
(71) Jäkle, F. *Dalton Trans.* **2007**, 2851-2858.
(72) Sundararaman, A.; Lalancette, R. A.; Zakharov, L. N.; Rheingold, A. L.; Jäkle, F. *Organometallics* **2003**, *22*, 3526-3532.
(73) Lin, J. C. Y.; Huang, R. T. W.; Lee, C. S.; Bhattacharyya, A.; Hwang, W. S.; Lin, I. J. B. *Chem. Rev.* **2009**, *109*, 3561-3598.
(74) Hashimoto, M.; Igawa, S.; Yashima, M.; Kawata, I.; Hoshino, M.; Osawa, M. *J. Am. Chem. Soc.* **2011**, *133*, 10348-10351.
(75) Gambarotta, S.; Strologo, S.; Floriani, C.; Chiesi-Villa, A.; Guastini, C. *Organometallics* **1984**, *3*, 1444-1445.
(76) Janssen, M. D.; Herres, M.; Spek, A. L.; Grove, D. M.; Lang, H.; van Koten, G. *Chem.Commun.* **1995**, 925-926.
(77) Janssen, M. D.; Köhler, K.; Herres, M.; Dedieu, A.; Smeets, W. J. J.; Spek, A. L.; Grove, D. M.; Lang, H.; van Koten, G. *J. Am. Chem. Soc.* **1996**, *118*, 4817-4829.
(78) Lang, H.; Köhler, K.; Rheinwald, G.; Zsolnai, L.; Büchner, M.; Driess, A.; Huttner, G.; Strähle, J. *Organometallics* **1999**, *18*, 598-605.
(79) Gurung, S. K.; Thapa, S.; Kafle, A.; Dickie, D. A.; Giri, R. *Org. Lett.* **2013**, *16*, 1264-1267.
(80) Zhao, N.; Zhang, J.; Yang, Y.; Chen, G.; Zhu, H.; H. W. Roesky *Organometallics* **2013**, *32*, 762-769.
(81) Bronner, C.; Wenger, O. *Dalton Trans.* **2011**, *40*, 12409-12420.
(82) To, W.-P.; Chan, K. T.; Tong, G. S. M.; Ma, C.; Kwok, W.-M.; Guan, X.; Low, K.-H.; Che, C.-M. *Angew. Chem. Int. Ed.* **2013**, *52*, 6648-6652.
(83) Kumar, R.; Linden, A.; Nevado, C. *Angew. Chem. Int. Ed.* **2015**, *127*, 14495-14498.
(84) Ragni, R.; Plummer, E. A.; Brunner, K.; Hofstraat, J. W.; Babudri, F.; Farinola, G. M.; Naso, F.; De Cola, L. *J. Mater. Chem.* **2006**, *16*, 1161-1170.
(85) Braun, T.; Cronin, L.; Higgitt, C. L.; McGrady, J. E.; Perutz, R. N.; Reinhold, M. *New J. Chem.* **2001**, *25*, 19-21.
(86) Schaub, T.; Fischer, P.; Steffen, A.; Braun, T.; Radius, U.; Mix, A. *J. Am. Chem. Soc.* **2008**, *130*, 9304-9317.
(87) Amarne, H.; Baik, C.; Murphy, S. K.; Wang, S. *Chem. - Eur. J.* **2010**, *16*, 4750-4761.
(88) Hofer, M.; Nevado, C. *Tetrahedron* **2013**, *69*, 5751-5757.
(89) Cai, X. Y.; Padmaperuma, A. B.; Sapochak, L. S.; Vecchi, P. A.; Burrows, P. E. *Appl. Phys. Lett.* **2008**, *92*.
(90) Marion, R.; Sguerra, F.; Di Meo, F.; Sauvageot, E.; Lohier, J.-F.; Daniellou, R.; Renaud, J.-L.; Linares, M.; Hamel, M.; Gaillard, S. *Inorg. Chem.* **2014**, *53*, 9181-9191.
(91) Costa, R. D.; Tordera, D.; Orti, E.; Bolink, H. J.; Schonle, J.; Graber, S.; Housecroft, C. E.; Constable, E. C.; Zampese, E. C. J. Mater. Chem. **2011**, *21*, 16108-16118..
(92) Kang, L.; Chen, J.; Teng, T.; Chen, X.-L.; Yu, R.; Lu, C.-Z. *Dalton Trans.* **2015**, *44*, 11649-11659.
(93) Kriechbaum, M.; List, M.; Berger, R. J. F.; Patzschke, M.; Monkowius, U. *Chem. Eur. J.* **2012**, *18*, 5506- 5509.
(94) Hobbollahi, E.; List, M.; Redhammer, G.; Zabel, M.; Monkowius, U. *Inorg. Chem. Commun.* **2016**, *65*, 24-27.
(95) Kriechbaum, M.; Winterleitner, G.; Gerisch, A.; List, M.; Monkowius, U. *Eur. J. Inorg. Chem.* **2013**, 5567-5575.
(96) Dolomanov, O. V.; Bourhis, L. J.; Gildea, R. J.; Howard, J. A. K.; Puschmann, H. *J. Appl. Crystallogr.* **2009**, *42*, 339-341.
(97) Sheldrick, G. *Acta Cryst. A* **2008**, *64*, 112-122.
(98) Bourhis, L. J.; Dolomanov, O. V.; Gildea, R. J.; Howard, J. A. K.; Puschmann, H. *Acta Cryst. A* **2015**, *71*, 59-75.
(99) Sheldrick, G. *Acta Cryst. A* **2015**, *71*, 3-8.
(100) Neese, F. *Wires Comput. Mol. Sci.* **2012**, *2*, 73-78.
(101) Perdew, J. P.; Tao, J. M.; Staroverov, V. N.; Scuseria, G. E. *J. Chem. Phys.* **2004**, *120*, 6898-6911.
(102) Tao, J. M.; Perdew, J. P.; Staroverov, V. N.; Scuseria, G. E. *Phys. Rev. Lett.* **2003**, 91.
(103) Adamo, C.; Barone, V. *J. Chem. Phys.* **1999**, *110*, 6158-6170.
(104) Ernzerhof, M.; Scuseria, G. E. *J. Chem. Phys.* **1999**, *110*, 5029-5036.
(105) Perdew, J. P.; Burke, K.; Ernzerhof, M. *Phys. Rev. Lett.* **1997**, *78*, 1396-1396.
(106) Perdew, J. P.; Burke, K.; Ernzerhof, M. *Phys. Rev. Lett.* **1996**, *77*, 3865-3868.
(107) Perdew, J. P.; Emzerhof, M.; Burke, K. *J. Chem. Phys.* **1996**, *105*, 9982-9985.
(108) Becke, A. D. *Phys. Rev. A* **1988**, *38*, 3098-3100.
(109) Perdew, J. P. *Phys. Rev. B* **1986**, *33*, 8822-8824.
(110) Weigend, F.; Ahlrichs, R. *Phys. Chem. Chem. Phys.* **2005**, *7*, 3297-3305.
(111) Schafer, A.; Horn, H.; Ahlrichs, R. *J. Chem. Phys.* **1992**, *97*, 2571-2577.
(112) Pantazis, D. A.; Chen, X. Y.; Landis, C. R.; Neese, F. *J. Chem. Theory Comput.* **2008**, *4*, 908-919.
(113) Schwerdtfeger, P.; Dolg, M.; Schwarz, W. H. E.; Bowmaker, G. A.; Boyd, P. D. W. *J. Chem. Phys.* **1989**, *91*, 1762-1774.
(114) Weigend, F. *Phys. Chem. Chem. Phys.* **2006**, *8*, 1057-1065.
(115) Grimme, S.; Ehrlich, S.; Goerigk, L. *J. Comput. Chem.* **2011**, *32*, 1456-1465.
(116) Grimme, S.; Antony, J.; Ehrlich, S.; Krieg, H. *J. Chem. Phys.* **2010**, *132*, 154104.
(117) Bergman, D. L.; Laaksonen, L.; Laaksonen, A. *J. Mol. Graph. Model.* **1997**, *15*, 301.
(118) Laaksonen, L. *J. Mol. Graphics* **1992**, *10*, 33.

TOC